

Privacy-Preserving Federated Learning for UAV-Enabled Networks: Learning-Based Joint Scheduling and Resource Management

Helin Yang, *Member, IEEE*, Jun Zhao, *Member, IEEE*,
Zehui Xiong, *Member, IEEE*, Kwok-Yan Lam, *Senior Member, IEEE*,
Sumei Sun, *Fellow, IEEE*, and Liang Xiao, *Senior Member, IEEE*

Abstract

Unmanned aerial vehicles (UAVs) are capable of serving as flying base stations (BSs) for supporting data collection, artificial intelligence (AI) model training, and wireless communications. However, due to the privacy concerns of devices and limited computation or communication resource of UAVs, it is impractical to send raw data of devices to UAV servers for model training. Moreover, due to the dynamic channel condition and heterogeneous computing capacity of devices in UAV-enabled networks, the reliability and efficiency of data sharing require to be further improved. In this paper, we develop an asynchronous federated learning (AFL) framework for multi-UAV-enabled networks, which can provide asynchronous distributed computing by enabling model training locally without transmitting raw sensitive data to UAV servers. The device selection strategy is also introduced into the AFL framework to keep the low-quality devices from affecting the learning efficiency and accuracy. Moreover, we propose an asynchronous advantage actor-critic (A3C) based joint device selection, UAVs placement, and resource management algorithm to enhance the federated convergence speed and accuracy. Simulation results demonstrate that our proposed framework and algorithm achieve higher learning accuracy and faster federated execution time compared to other existing solutions.

H. Yang, Z. Xiong, J. Zhao, and K. Y. Lam are with the School of Computer Science and Engineering, and Strategic Centre for Research in Privacy-Preserving Technologies, Nanyang Technological University, Singapore 639798 (e-mail: hyang013@e.ntu.edu.sg, zxiong002@e.ntu.edu.sg, junzhao@ntu.edu.sg, kwokyan.lam@ntu.edu.sg).

S. Sun is with the Institute for Infocomm Research, Agency for Science, Technology, and Research, Singapore 138632 (e-mail: sunsm@i2r.a-star.edu.sg).

L. Xiao is with the Department of Information and Communication Engineering, Xiamen University, Xiamen 361005, China (e-mail: lxiao@xmu.edu.cn).

Index Terms—Unmanned aerial vehicle, data sharing, asynchronous federated learning, scheduling, resource management, asynchronous advantage actor-critic.

I. INTRODUCTION

With the rapid deployment of fifth-generation (5G) and beyond wireless networks, unmanned aerial vehicles (UAVs) have been emerged as a promising candidate paradigm to provide communication and computation services for ground mobile devices in sport stadiums, outdoor events, hot spots, and remote areas [1]-[3], where aerial base stations (BSs) or servers can be mounted on UAVs. Given the benefits of agility, flexibility, mobility, and beneficial line-of-sight (LoS) propagation, UAV-enabled networks have been widely applied in quick-response wireless communications, data collection, artificial intelligence (AI) model training, and coverage enhancement [1]. Correspondingly, UAV-assisted computation and communication tasks have attracted significant interest recently in 5G and beyond wireless networks [3].

Again, deploying UAVs as flight BSs is able to flexibly to collect data and implement AI model training for ground devices, but it is impractical for a large number of devices to transmit their raw data to UAV servers due to the privacy concern and limited communication resources for data transmission [4]. Moreover, as the energy capacity, storage, and computational ability of UAVs are limited, it is still challenging for UAVs to process/training a large amount of raw data [1], [2], [4]. In face of the challenges, federated learning (FL) [5], [6] emerges as a promising paradigm aiming to protect device privacy by enabling devices to train AI model locally without sending their raw data to a server. Instead of training AI model at the data server, FL enables devices to execute local training on their own data, which generally uses the gradient descent optimization method [7].

By using FL, UAVs can perform distributed AI tasks for ground mobile devices without relying on any centralized BS, and devices also do not need to send any raw data to UAVs during the training [4]. In particular, wireless devices use their respective local datasets to train AI models, and upload the local model parameters to an FL UAV server for model aggregation. After collecting the local model parameters from devices, the UAV server then aggregates the updated model parameters before broadcasting the parameters to associated devices for another round of local model training. During the process, keeping raw data at devices not only preserves privacy but also reduces network traffic congestion. A number of rounds are performed until a target learning accuracy is obtained. In essence, FL allows UAV-enabled wireless networks to train AI models in an efficient way, compared with centralized cloud-centric frameworks. However, since the parameters of AI models in FL need to be exchanged between UAV servers

and devices, the FL convergence and task consensus for UAV servers will inevitably be affected by transmission latency [4]. In addition, due to the mobility of UAVs and devices, dynamic channel conditions can negatively affect the FL convergence [8]. Moreover, UAV servers are generally limited in terms of computation and energy resources, resulting in the necessity of design for efficient scheduling and management approaches to minimize the FL execution time [1], [4], [9]. Hence, the aforementioned challenges pertaining to FL specifically that need to be investigated for large scale implementation of efficient FL in UAV-enabled wireless networks.

A. Related Works

In recent years, implementing FL in wireless networks has attracted many research efforts, and lots of studies have presented their studies that how to adopt FL to improve the learning efficiency [10]-[17]. Tran *et al.* [10] formulated an FL framework over a wireless network as an optimization problem that minimizes the sum of FL aggregation latency and total device energy consumption. In addition, the frequency of global aggregation under different resource constraints (i.e., device central processing unit (CPU), transmission delay, and model accuracy) has been optimized in [11], [12]. However, in [10]-[12], due to the limited wireless spectrum, it is difficult to implement practical wireless FL applications when all mobile devices are involved in each aggregation iteration. Hence, some studies proposed to apply the device selection/scheduling scheme to improve the convergence speed of FL [13]-[16]. The authors in [13] studied the relationship between the number of rounds and different device scheduling policies (i.e., random scheduling, round-robin, and proportional fair), and compared their performances by simulations. A deep reinforcement learning (DRL)-based device selection algorithm was proposed to enhance the reliability and efficiency in an asynchronous federated learning manner [14]. Shi *et al.* [9] formulated a joint channel allocation and device scheduling problem to study the convergence speed of FL, but the solution to the problem is not globally optimized. In [15], the authors introduced a novel hierarchical federated edge learning framework, and a joint device and resource scheduling algorithm was proposed to minimize both the system energy and FL execution delay cost. A greedy scheduling scheme was proposed in [16] that manages a part of clients to participate in the global FL aggregation according to their resource conditions. However, the work [16] failed to verify the effectiveness of the scheme in the presence of dynamic channels and computation capabilities.

To the best of our knowledge, there are several studies [4], [8], [9], [18]-[22] that investigated how to apply FL to improve AI model learning efficiency in UAV-enabled communication scenarios. For instance, the authors in [8], [18] developed a novel framework to enable FL

within UAV swarms, and a joint power allocation and flying trajectory scheme was proposed to improve the FL learning efficiency [8]. Lim *et al.* [19] proposed an FL-based sensing and collaborative learning approach for UAV-enabled internet of vehicles (IoVs), where UAVs collect data and train AI model for IoVs. In addition, Ng *et al.* [20] presented the use of UAVs as flight relays to support the wireless communications between IoVs and the FL server, hence enhancing the accuracy of FL. Shiri *et al.* [9] adopted FL and mean-field game (MFG) theory to address the online path design problem of massive UAVs, where each UAV can share its own model parameters of AI with other UAVs in a federated manner. The work in [4] provided discussions of several possible applications of FL in UAV-enabled wireless networks, and introduced the key challenges, open issues, and future research directions therein. To preserve the privacy of devices, a two-stage FL algorithm among the devices, UAVs, and heterogeneous computing platform was proposed to collaboratively predict the content caching placement in a heterogeneous computing architecture [21]. Furthermore, the authors in [22] introduced a blockchain-based collaborative scheme in the proposed secure FL framework for UAV-assisted mobile crowdsensing, which effectively prevents potential security and privacy threats from affecting secure communication performance. However, most of the studies [4], [8], [9], [18]-[22] did not jointly consider the importance of the tasks (i.e., learning accuracy and execution time) of FL that UAVs perform, and the optimal dynamic scheduling and resource management of UAVs to complete the tasks, subject to the resource constraints of UAVs and different computational capabilities of devices.

Joint management of both UAVs trajectory (or UAVs placement) and resource management has been widely studied to optimize the network performance, such as in [23]–[28]. In [23] and [24], a joint optimization for user association, resource allocation, and UAV placement was studied in multi-UAV wireless networks, to guarantee the quality of services (QoS) of mobile devices. However, the conventional optimization methods adopted in [23], [24] may be not effective as the UAVs-enabled environment are dynamic and complex. To address this issue, reinforcement learning (RL) or DRL has been adopted to learn the decision-making strategy [25]–[28]. The authors in [25], [26] applied the multi-agent DRL algorithm to address the joint UAVs trajectory and transmit power optimization problem, and also demonstrated the effectiveness of multi-agent DRL algorithms compared with baseline schemes. Considering the fact that UAVs have continuous action spaces (i.e., trajectory, location, and transmit power), Zhu *et al.* [27] proposed an actor-critic (AC)-based algorithm to jointly adjust UAV's transmission control and three-dimensional (3D) flight to maximize the network throughput over continuous action spaces. Similarly, in [28], the authors adopted the AC-based algorithm to optimize the device association,

resource allocation, and trajectory of UAVs in dynamic environments. However, to the best of our knowledge, there are no studies applying RL or DRL to achieve the implementation of FL for the UAVs-enabled wireless network, and optimize the FL convergence or accuracy by jointly designing scheduling and resource management.

B. Contributions and Organization

Motivated by the aforementioned challenges, this paper first develops an asynchronous federated learning (AFL) to achieve fast convergence speed and high learning accuracy for multi-UAV-enabled wireless networks. The proposed framework can enable mobile devices to train their AI models locally and asynchronously upload the model parameters to UAV servers for model aggregation without uploading the raw private data, which reduces communication cost and privacy threats, as well as improves the round efficiency and model accuracy. Considering the dynamic environment and different computational capabilities of devices, we also propose an asynchronous advantage actor-critic (A3C)-based joint device selection, UAVs placement, and resource management algorithm to further enhance the overall federated execution efficiency and model accuracy. The main contributions of this paper are summarized as follows.

- We develop a novel privacy-preserving AFL framework for a multi-UAV-enabled wireless network to aggregate and update the AI model parameters in an asynchronous manner, where the mobile devices with high communication and computation capabilities are selected to participate in global aggregation instead of waiting for all associated devices to accomplish their local model update.
- We propose an A3C-based joint device selection, UAVs placement, and resource management algorithm to further minimize the federated execution time and learning accuracy loss under dynamic environments as well as large-scale continuous action spaces.
- We conduct extensive simulations to demonstrate that the proposed AFL framework and A3C-based algorithm can significantly improve the FL model accuracy, convergence speed, and federated execution efficiency compared to other baseline solutions under different scenarios.

Organization: The remainder of this paper is organized as follows. The system model and problem formulation are provided in Section II. Section III proposes the AFL framework and A3C-based algorithm for UAV-enabled wireless networks. Simulation results and analysis are provided in Section IV, and the paper is concluded in Section V.

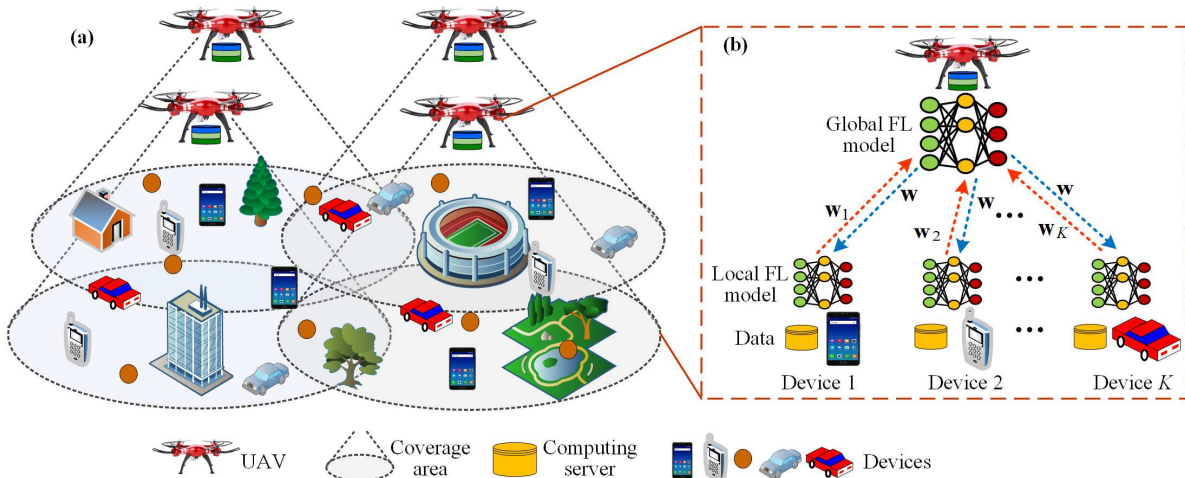


Fig. 1. Federated learning-based UAV-enabled wireless networks.

II. SYSTEM MODEL AND PROBLEM FORMULATION

We consider an FL instance consisting of a number of ground devices, which are associated with several parameter servers residing at multiple UAVs in the sky. As shown in Fig. 1, the multi-UAV-enabled network consists of N UAVs and K single-antenna devices, denoted by $\mathcal{N} = \{1, \dots, N\}$ and $\mathcal{K} = \{1, \dots, K\}$, respectively. In practical wireless networks, the ground BS may face congestion due to a BS malfunction, or a temporary festival or a big sport event, and even ground BS may fail to provide coverage in some remote areas. In this case, the deployment of UAVs has been emerged as a potential technique for providing wireless coverage for ground devices. As illustrated in Fig. 1, mobile devices are randomly located on the ground, and multiple UAVs fly in the sky to provide wireless services for them by using frequency division multiple access (FDMA). Here, the unity frequency reuse (UFR) design is employed in multi-UAV networks to enhance the spectrum utilization, where the communication band is reused across all cells with each cell being associated with one UAV [23]-[26].

In the FL instance, each device has its own personal dataset and it is willing to upload a part of inflammation (i.e., AI model parameters) to its associated UAV server in a privacy-preserving manner. In addition, devices involved in a common computing task (e.g., training a classification model) are more likely to work with others together to finish the task collaboratively, by adopting AI techniques. These devices will update their own local AI model parameters to associated UAV servers for global model aggregation. Each device processes the local model training based on its local raw dataset without sharing the raw data with other devices, to protect

the privacy of data providers. After completing local model training, each device will send its local model parameters to its associated UAV server by the uplink communication channel, and the corresponding UAV server aggregates the local parameters from the selected devices before broadcasting the aggregated global parameters to the devices by the downlink communication channel.

For the FL aggregation, communication and computation resource optimization (related to both the computation capability and communication capability) is necessary to realize the implementation of model aggregation, such as local computation, communication [5], [6], and global computation at both the devices and the UAV servers. The computation capacity of each device or each UAV server is captured by the CPU capability, learning time, and learning accuracy. The communication capacity can be characterized in the forms of the available transmission rate and transmission latency. It is worth noting that both the computation and communication capabilities may vary at different time slots due to different computing tasks and mobility of UAVs or devices. Hence, this paper also focuses on joint device selection, UAVs placement design, and resource management to enhance the leaning efficiency and accuracy of FL.

A. FL Model

This subsection briefly investigates the basics of FL in multi-UAV-enabled networks. Hereinafter, the considered AI model that is trained on each device's training dataset is called local FL model, while the FL model that is built by each UAV server employing local model parameter inputs from its selected devices is called global FL model.

Let \mathbf{w}_n denote the model parameters which is related to the global model of the n -th UAV server, let \mathbf{w}_k denote the local model parameters of the k -th device, and let \mathcal{D}_k denote the set of training dataset used at the k -th device. Accordingly, if the k -th device is associated with the n -th UAV server, we introduce the loss function $f(\mathbf{w}_n; \mathbf{s}_{k,i}, z_{k,i})$ to quantify the FL performance error over the input data sample vector $\mathbf{s}_{k,i}$ on the learning model \mathbf{w} and the desired output scalar $z_{k,i}$ for each input sample i at the k -th device. For the k -th device, the sum loss function on its training dataset \mathcal{D}_k can be expressed as [5], [6]

$$F_k(\mathbf{w}_n) = \frac{1}{|\mathcal{D}_k|} \sum_{i \in \mathcal{D}_k} f(\mathbf{w}_n; \mathbf{s}_{k,i}, z_{k,i}), \quad \forall k \in \mathcal{K}, \quad (1)$$

where $|\mathcal{D}_k|$ is the cardinality of set \mathcal{D}_k . Accordingly, at the n -th UAV server, the average global loss function with the distributed local datasets of all selected devices is defined as [5], [6]

$$F(\mathbf{w}_n) \triangleq \sum_{k \in \mathcal{K}_n} \frac{|\mathcal{D}_k| F_k(\mathbf{w}_n)}{|\mathcal{D}_n|} = \frac{1}{|\mathcal{D}_n|} \sum_{k \in \mathcal{K}_n} \sum_{i \in \mathcal{D}_k} f(\mathbf{w}_n; \mathbf{s}_{k,i}, z_{k,i}), \quad (2)$$

where $|\mathcal{D}_n| = \sum_{k \in \mathcal{K}_n} |\mathcal{D}_k|$ is the sum data samples from all selected devices at the n -th UAV-enabled cell, and \mathcal{K}_n is the set of the devices associated with the n -th UAV server with $K_n = |\mathcal{K}_n|$ being the number of the selected devices. The objective of the FL task is to search for the optimal model parameters at the n -th UAV server that minimizes the global loss function as [5], [6]

$$\mathbf{w}_n^* = \arg \min F(\mathbf{w}_n), \quad \forall n \in \mathcal{N}. \quad (3)$$

Note that $F(\mathbf{w}_n)$ cannot be directly computed by employing the raw datasets from selected devices, for the sake of protecting the information privacy and security of each device. Hence, the problem in (3) can be addressed in a distributed manner. We pay attention to the FL model-averaging implementation in the subsequent exposition while the same principle is generally adopted to realize alternative implementation according to the gradient-averaging method [5], [6].

B. Communication Model

Different from the propagation of ground communications, the air-to-ground or ground-to-air channel mainly depends on the propagation environments, transmission distance, and elevation angle [1]-[3]. Similar to existing works [23]-[28], the UAV-to-device or device-to-UAV communication channel link is modeled by a probabilistic path loss model, where both the LoS and non-LoS (NLoS) links are taken into account. The LoS and NLoS path loss in dB from the n -th UAV server to the k -th device can be given by

$$l_{n,k}^{\text{LoS}} = 20 \log(4\pi f_c d_{n,k}/c) + \eta^{\text{LoS}}, \quad (4)$$

$$l_{n,k}^{\text{NLoS}} = 20 \log(4\pi f_c d_{n,k}/c) + \eta^{\text{NLoS}}, \quad (5)$$

respectively, where f_c and c denote the carrier frequency and the speed of light, respectively. $d_{n,k}$ is the transmission distance from the n -th UAV server to the k -th device, given by $d_{n,k} = [(x_n - x_k)^2 + (y_n - y_k)^2 + h_n^2]^{1/2}$, where $\Theta_n = (x_n, y_n, h_n)$ denotes the location of the n -th UAV server, $\Theta_k = (x_k, y_k)$ is the location of the k -th device, and h is the height of UAV servers in the sky, and we assume that all UAVs have the same height. η^{LoS} and η^{NLoS} are the mean additional losses for the LoS and NLoS links due to the free space propagation loss, respectively, as defined in [29]. In the communication model, the probability of LoS connection between the n -th UAV server and the k -th device is expressed as

$$P_{n,k}^{\text{LoS}} = \frac{1}{1 + \xi_1 \exp(-\xi_2(\theta_{n,k} - \xi_1))}, \quad (6)$$

where ξ_1 and ξ_2 are constant values which depend on the carrier frequency and UAV network environment, and $\theta_{n,k}$ is the elevation angle from UAV n to device k (in degree): $\theta_{n,k} = \frac{180}{\pi} \cdot \sin^{-1}\left(\frac{h_n}{d_{n,k}}\right)$. Furthermore, the probability of NLoS is $P_{n,k}^{\text{NLoS}} = 1 - P_{n,k}^{\text{LoS}}$. In this context, the probabilistic path loss between the n -th UAV and the k -th device is given by

$$l_{n,k} = P_{n,k}^{\text{LoS}} \cdot l_{n,k}^{\text{LoS}} + P_{n,k}^{\text{NLoS}} \cdot l_{n,k}^{\text{NLoS}}. \quad (7)$$

We assume that orthogonal frequency-division multiple access (OFDMA) technique is used for uplink channel access, where each UAV-enabled cell has M orthogonal uplink subchannels and these subchannels are reused across all cells. Note that the total uplink bandwidth is divided into M orthogonal subchannels, denoted by $\mathcal{M} = \{1, \dots, M\}$. In this case, each UAV server will suffer inter-cell interference (ICI) from other nearby devices associated by other cells on the same spectrum band. Hence, according to the path loss model, when the k -th device is associated with the n -th UAV server, the received signal-to-interference plus-noise-ratio (SINR) over the allocated subchannel m at the n -th UAV server in the uplink is characterized as

$$SINR_{n,k,m}^{\text{U}} = \frac{P_{k,m}^{\text{U}} 10^{-l_{n,k}/10}}{\sum_{k' \in \mathcal{K}, k' \neq k} P_{k',m}^{\text{U}} 10^{-l_{n,k'}/10} + \sigma^2}, \quad (8)$$

where $P_{k,m}^{\text{U}}$ is the transmit power of the k -th device allocated on the m -th subchannel, and σ^2 denotes the power of the Gaussian noise. Furthermore, $\sum_{k' \in \mathcal{K}, k' \neq k} P_{k',m}^{\text{U}} 10^{-l_{n,k'}/10}$ is the ICI received at UAV server n over the m -th subchannel which is generated from nearby devices associated by other cells. Accordingly, the achievable uplink data rates (in bit/s) for the k -th device over the allocated subchannels can be expressed as

$$R_k^{\text{U}} = B_{\text{sub}} \sum_{m=1}^M (\chi_{n,k,m} \log_2(1 + SINR_{n,k,m}^{\text{U}})), \quad (9)$$

where $B_{\text{sub}} = B^{\text{U}}/M$ is the bandwidth of each uplink subchannel with B^{U} being the total bandwidth in uplink, and $\chi_{n,k,m}$ is the uplink subchannel allocation indicator, $\chi_{n,k,m} \in \{0, 1\}$; $\chi_{n,k,m} = 1$ shows that the k -th device is associated with the n -th UAV server on the m -th subchannel ; otherwise, $\chi_{n,k,m} = 0$.

For the downlink channel, we assume that each UAV server occupies a given downlink channel to broadcast the global model parameters to its associated devices. As the deployment of multiple UAVs in the sky, devices located in the overlapped areas will also suffer ICI from other nearby

UAV servers on the same spectrum band. Then, when the k -th device is associated with the n -th UAV server, its received SINR in the downlink can be expressed as

$$SINR_{n,k}^D = \frac{P_n^D 10^{-l_{n,k}/10}}{\sum_{n' \in \mathcal{N}, n' \neq n} P_{n'}^D 10^{-l_{n,k}/10} + \sigma^2}. \quad (10)$$

where P_n^D is the transmit power of the n -th UAV server. Accordingly, the achievable downlink data rate at the k -th device is given by

$$R_k^D = B^D \log_2(1 + SINR_{n,k}^D), \quad (11)$$

where B^D is the bandwidth in the downlink.

C. FL Model Update Latency Analysis

Local/Global Model Update Latency: Define C_k and C_n as the number of CPU cycles used for training model on one sample data at the k -th device and n -th UAV server, respectively. Let f_k and f_n denote the computation capability (CPU cycles/s) of device k and UAV server n , respectively, where $f_k \in (f_k^{\min}, f_k^{\max})$ with f_k^{\min} and f_k^{\max} being the minimum and maximum CPU computation capabilities of device k , respectively. Accordingly, the local model computation latency of device k and the global model aggregation latency of UAV server n at the t -th time slot are respectively given by

$$T_k^{\text{Loc},t} = |\mathcal{D}_k| C_k / f_k, \quad \forall k, \quad (12)$$

$$T_n^{\text{Glo},t} = |\mathcal{D}_n| C_n / f_n, \quad \forall n. \quad (13)$$

Global FL Model Broadcast Latency: Let L_n denote the number of bits required for each UAV server n to broadcast the global model parameters to the associated devices. For the n -th UAV server, the global model parameters broadcast latency is expressed as

$$T_n^{\text{D},t} = L_n / R_n^{\text{D},t}, \quad \forall n. \quad (14)$$

Local FL Model Upload Latency: Let L_k denote the number of bits needed for each device k to upload its local model parameters to its associated UAV server. For the k -th device, the local model parameters upload latency can be given by

$$T_k^{\text{U},t} = L_k / R_k^{\text{U},t}, \quad \forall k. \quad (15)$$

The one round time for scheduling the k -th device is comprised of local model update latency, uplink local model upload latency, global model aggregation latency, and downlink global model

broadcast latency. Therefore, the total time cost for scheduling the FL-model of the k -th device at one round can be given by

$$T_k^t = T_k^{\text{Loc},t} + T_n^{\text{Glo},t} + T_k^{\text{D},t} + T_k^{\text{U},t}, \quad \forall k. \quad (16)$$

D. Problem Formulation

In UAV-enabled networks, the various computation capacities of devices and the time-varying communication channel conditions play an important role on the implementation of FL global aggregation. It is desirable to select the devices with high computation capability, communication capability, and accurate learned models. In addition, it is necessary to schedule UAVs' locations to provide the best channel gains for communication services, and manage the radio and power resources to improve the communication data rate for AI model parameters upload and broadcast. Thus, we aim to select a subset of devices, design UAVs' locations, manage subchannel and transmit power resources to minimize the FL model execution time and the learning accuracy loss. In the n -th UAV-enabled cell, we define the execution time cost as

$$c_n^{\text{Time}}(t) = \frac{1}{K_n} \sum_{k=1}^{K_n} T_k^t, \quad \forall n, \quad (17)$$

where K_n is the number of devices selected by the n -th UAV server for the federated model aggregation. In addition, the learning accuracy loss can be defined as

$$c_n^{\text{Loss}}(t) = \frac{1}{|\mathcal{D}_n|} \sum_{k \in \mathcal{K}_n} \sum_{i \in \mathcal{D}_k} f(\mathbf{w}_n; \mathbf{s}_{k,i}, z_{k,i}), \quad \forall n. \quad (18)$$

In the network, the learning accuracy loss is measured at the end of each time slot.

Given the aforementioned system model, our objective is to minimize the weighted sum of one-round FL model execution time and learning accuracy loss. Targeting at learning acceleration and efficiency, it is desirable to select a subset of devices with high computation capability, place the UAVs' locations with best channel quality, as well as manage both subchannel and power resources. Hence, the optimization problem can be formulated as follows

$$\begin{aligned} & \min_{\Theta_n, \rho, \chi, P_n^{\text{D}}} (\lambda c_n^{\text{Time}}(t) + (1 - \lambda) c_n^{\text{Loss}}(t)), \quad \forall n \\ & \text{s.t. } \text{a) } \rho_{n,k} \in \{0, 1\}, \chi_{n,k,m} \in \{0, 1\}, \forall k, m, \\ & \quad \text{b) } \sum_{n \in \mathcal{N}} \rho_{n,k} \leq 1, \forall k, \\ & \quad \text{c) } \sum_{k \in \mathcal{K}} \sum_{m \in M} \chi_{n,k,m} \leq M, \\ & \quad \text{d) } 0 \leq P_n^{\text{D}} \leq P_n^{\text{max}}, \\ & \quad \text{e) } 0 \leq f_k \leq f_k^{\text{max}}, \forall k, \end{aligned} \quad (19)$$

where $\boldsymbol{\rho} = [\rho_{n,1}, \dots, \rho_{n,K}]^T$ and $\boldsymbol{\chi} = [\chi_{n,1,1}, \dots, \chi_{n,1,M}, \chi_{n,2,1}, \dots, \chi_{n,2,M}, \dots, \chi_{n,K,M}]$, P_n^{\max} is the maximum transmit power of UAV server n , and $\lambda \in [0, 1]$ is a constant weight parameter which is used to balance the one-round execution time c_n^{Time} and the learning accuracy loss c_n^{Loss} . Constraint (19b) indicates that each device can only associate one UAV server to preform model aggregation. Constraint (19c) is used to ensure the maximum number of available subchannels of each UAV-enabled cell. Constraint (19d) ensures the maximum transmit power of UAV server n in the downlink. Constraint (19d) represents the computation capacity range of devices. We would like to mention that for the resource management issue, we focus our study on the uplink subchannel allocation since the global model parameters at each UAV server are broadcast by a given downlink band. In addition, we also investigate the power allocation at each UAV server by assuming that the transmit power of each device is given.

III. ASYNCHRONOUS FEDERATED REINFORCEMENT LEARNING SOLUTION

The optimization problem formulated in (19) is challenging to tackle as it is a non-convex combination and NP-hard problem. In addition, the time-varying channel condition and different computation capacities of devices result in dynamic open and uncertain characteristics, which increases the difficulty of addressing the optimization problem. Model-free RL is one of the dynamic programming technique which is capable of tackling the decision-making problem by learning an optimized policy in dynamic environments [30]. Thus, RL is introduced to implement the self-scheduling based FL aggregation process in multi-UAV-enable networks.

Moreover, traditional FL models mostly use a synchronous learning framework to update the model parameters between the UAV servers and client devices, which inherently have several key challenges. Firstly, due to the mobility and different computation capacities of mobile devices, it is difficult to maintain continuous synchronized communication between UAV servers and client devices. Secondly, each UAV server needs to wait for all selected devices to finish their local results before aggregating the model parameters, which consequently increases the global learning delay with low round efficiency. Furthermore, a part of the action (i.e., transmission power and horizontal locations of UAVs) in our joint placement design and resource management optimization problem have continuous spaces. Therefore, we propose an asynchronous advantage actor-critic-based asynchronous federated learning algorithm (called A3C-AFL) to address the aforementioned challenges, and the corresponding framework is provided with the following extensive details in this section.

The proposed A3C-AFL framework consists of three phases: device selection, UAVs placement as well as resource management; local training; and global aggregation, as illustrated in Fig. 2.

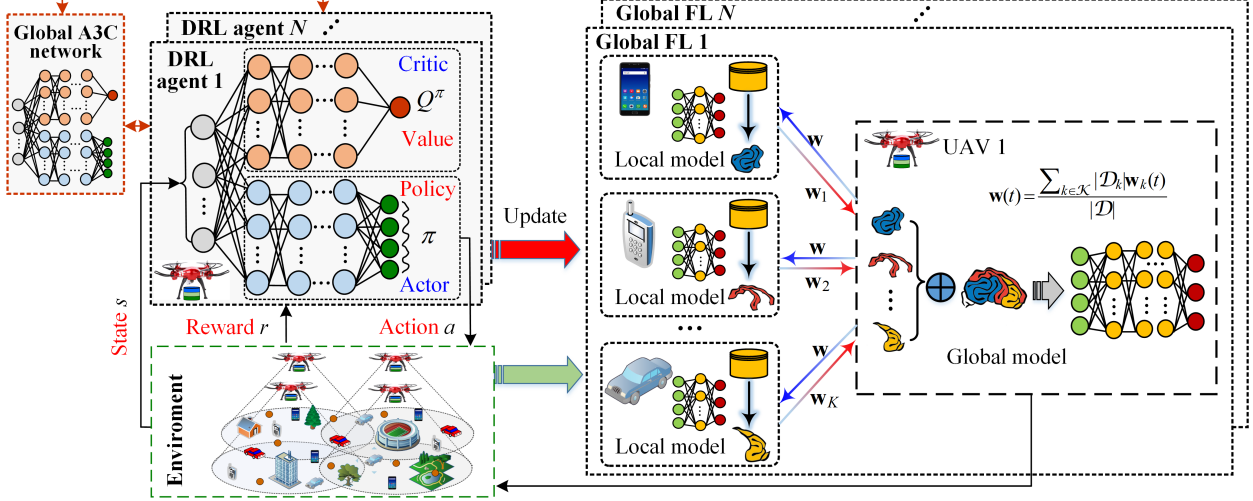


Fig. 2. The framework of A3C-AFL in UAV-enabled networks.

The strategy of the device selection, UAV placement design, and resource management can be achieved by using the A3C algorithm. Then, the selected devices in each UAV-enabled cell perform local training and periodically upload their local model parameters to their corresponding associated UAV server for global aggregation. Finally, each UAV server broadcasts the updated global model parameters to the associated devices.

- Device Selection, UAVs Placement, and Resource Management:** To improve the learning efficiency and accuracy, each UAV server selects the devices with high computation and communication capacities to perform federated model parameters update. Then, the joint UAVs placement design and resource management are implemented to minimize the execution time. This phase is implemented by adopting the A3C-based algorithm [31], which will be elaborated in Section III.B.
- Local Training:** At the t -th global communication round, after receiving the global model parameters $\mathbf{w}_n(t-1)$ from the associated UAV server, each selected device k trains its local model parameters $\mathbf{w}_k(t)$ based on its dataset \mathcal{D}_k by calculating the local stochastic gradient descent $\nabla F_k(\mathbf{w}_n(t-1))$, i.e.,

$$\mathbf{w}_k(t) = \mathbf{w}_n(t-1) - \eta \nabla F_k(\mathbf{w}_n(t-1)), \quad (20)$$

where $\eta > 0$ denotes the learning step size and ∇ is the gradient operator. After updating the parameters $\mathbf{w}_k(t)$, each device k uploads its trained local model parameters $\mathbf{w}_k(t)$ to its associated UAV server for further FL model aggregation.

- **Global Aggregation:** Each UAV server n (aggregator) retrieves the uploaded local FL model parameters from its selected devices and implements the global model aggregation through averaging and updating the global model parameters $\mathbf{w}_n(t)$ as follows

$$\mathbf{w}_n(t) = \frac{\sum_{k \in \mathcal{K}_n} |\mathcal{D}_k| \mathbf{w}_k(t)}{|\mathcal{D}_n|}. \quad (21)$$

The model parameters update process involves the iteration between (20) and (21) until the FL model converges.

A. Modeling of Reinforcement Learning Environment

We formulate the combinatorial optimization problem (19) as a Markov decision process (MDP), i.e., $\langle \mathcal{S}, \mathcal{A}, \mathcal{P}, r \rangle$, where \mathcal{A} , \mathcal{S} , \mathcal{P} , and r are network state space, action space, state transition probability, and reward function, respectively. In multi-UAV-enabled networks, UAV servers are considered as multiple agents to observe the environment and try to maximize the expected sum reward. Then, we use RL to tackle the device selection, UAVs placement, and resource management problem (19) in the federated learning scenario. All of the multiple agents iteratively update their policies based on their observations by interacting with the network environment. According to the aforementioned MDP, i.e., $\langle \mathcal{S}, \mathcal{A}, \mathcal{P}, r \rangle$, the corresponding elements in MDP are described as below:

State Space: At each time slot t , the network state $s_n(t) \in \mathcal{S}$ of each UAV server n for characterizing the environment is comprised of the following several parts: horizontal location of the n -th UAV server $\Theta_n(t) = (x_n(t), y_n(t))$; device selection indicators at the n -th UAV-enabled cell, $\{\rho_{n,k}(t-1)\}_{k \in \mathcal{K}_n}$; the subchannel allocation state $\{\chi_{n,k,m}(t-1)\}_{k \in \mathcal{K}_n}$; locations of selected devices, $\{\Theta_k(t) = (x_k(t), y_k(t))\}_{k \in \mathcal{K}_n}$; the remaining payload needs to be transmitted, $\{L_k(t-1)\}_{k \in \mathcal{K}_n}$ and $L_n(t-1)$. According to the above definitions, in the multi-agent RL model, the network state of the n -th UAV server at time slot t can be expressed by

$$s_n(t) = \left\{ \Theta_n(t), L_n(t-1), \left\{ \Theta_k(t), \rho_{n,k}(t-1), \chi_{n,k,m}(t-1), L_k(t) \right\}_{k \in \mathcal{K}_n} \right\}, \quad (22)$$

and the network state of all UAV servers is given by $s_t = \left\{ \left\{ s_n(t) \right\}_{n \in \mathcal{N}} \right\}$.

Action Space: At the t -th time slot, each agent n (i.e., UAV server n) selects its corresponding action $a_n(t) \in \mathcal{A}$ according to the observed state $s_n(t)$, where $a_n(t)$ consists of the horizontal position $\Theta_n(t) = (x_n(t), y_n(t))$, the device selection indicators $\{\rho_{n,k}(t)\}_{k \in \mathcal{K}_n}$, the subchannel allocation indicators $\{\chi_{n,k,m}(t)\}_{k \in \mathcal{K}_n}$, and the transmit power allocation level $P_n^D(t)$, that is

$$a_n(t) = \left\{ \Theta_n(t), P_n^D(t), \left\{ \rho_{n,k}(t), \chi_{n,k,m}(t) \right\}_{k \in \mathcal{K}_n} \right\}, \quad (23)$$

and the action of all UAV servers is given by $a_t = \{\{a_n(t)\}_{n \in \mathcal{N}}\}$. At the end of each time slot t , each UAV server moves to an updated horizontal position, updates the device association indicators, allocates subchannel and power resources to devices, respectively.

State Transition Function: Let $\mathcal{P}(s_{t+1}|s_t, a_t)$ denote the transition probability of one UAV server entering a new state s_{t+1} , after executing an action a_t at the current state s_t .

Policy: Let π denote the policy function, which is a mapping from perceived states with the probability distribution over actions that the agent can select in those states, $\pi(a|s) = \mathcal{P}(a|s)$.

Reward Function: In the context of minimizing the one round FL model execution time and learning accuracy loss, the reward function r_t is designed to evaluate the quality of a learning policy under the current state-action pair (s_t, a_t) . In this paper, we design a reward function that can capture the federated execution time and learning accuracy loss. According to the objective function in (19), the presented reward function of the n -th agent (i.e., UAV server n) at one time step is expressed as

$$r_n(s_t, a_t) = -(\lambda c_n^{\text{Time}}(t) + (1 - \lambda)c_n^{\text{Loss}}(t)). \quad (24)$$

The objective of the UAV-enabled network is to minimize the execution time and learning accuracy loss in FL. For the MDP model, the objective is to search for an action a which is capable of maximizing the cumulative reward (minimize the total cumulative execution time and learning accuracy loss), given by

$$U_t = \sum_{\tau=0}^{\infty} \gamma^\tau r(s_{t+\tau}, a_{t+\tau}), \quad (25)$$

where γ denotes the discount factor.

B. Multi-Agent A3C Algorithm

In multi-UAV-enabled networks, the spaces of both state and action are large, and hence combining deep learning and RL, i.e., DRL algorithms (e.g., deep Q-learning and deep deterministic policy gradient), are effective for handling the large-scale decisions making problems [30]. These algorithms generally adopt experience replay to improve learning efficiency. However, experience replay requires enough memory space and computation resources to guarantee the learning accuracy, and it only uses the data generated through old policy to update the learning process [31]. The negative issues of the aforementioned DRL algorithms motivate us to search for a better algorithm, A3C (asynchronous advantage actor-critic).

Different from a classical AC algorithm with only one learning agent, A3C is capable of enabling asynchronous multiple agents (i.e., UAV servers) to parallelly interact with their environments and achieve different exploration policies. In A3C, the actor network generally adopts policy gradient schemes to select actions under a given parameterized policy $\pi(a|s; \theta_a) = \mathcal{P}(a|s, \theta_a)$ with a set of actor parameters θ_a , and then updates the parameters by the gradient-descent methods. The critic network uses an estimator of the state value function $V^\pi(s_t; \theta_c)$ to qualify the expected return under a certain state s with a set of critic parameters θ_c .

Each UAV server acts as one agent to evaluate and optimize its policy based on the value function, which is defined as the expected long-term cumulative reward achieved over the entire learning process. Here, we defined two value functions, called state value function and state-action value function, where the former one is the expected return under a given policy π while the latter one is the expected return under a given policy π after executing action a in state s . These two functions are respectively expressed as

$$V^\pi(s_t; \theta_c) = \mathbb{E} \{U_t | s_t = s, \pi\}, \quad (26)$$

$$Q^\pi(s_t, a_t) = \mathbb{E} \{U_t | s_t = s, a_t = a, \pi\}, \quad (27)$$

where $\mathbb{E}\{\cdot\}$ is the expectation.

A3C adopts the multi-step reward to update the parameters of the policy in the actor network and the value function in the critic network [31]. Here, the i -step reward is defined as [31]

$$U_t = \sum_{i=0}^{\tau-1} \gamma_i r(s_{t+i}, a_{t+i}) + \gamma_\tau V^\pi(s_{t+\tau}; \theta_c). \quad (28)$$

Similar to the AC framework, A3C also adopts policy gradient schemes to perform parameters update which may cause high variance in the critic network. In order to address this issue, an advantage function $A(s, a) = Q^\pi(s, a) - V^\pi(s; \theta_c)$ is employed to replace $Q^\pi(s, a)$ in the policy gradient process. Since $Q^\pi(s, a)$ cannot be determined in A3C [31], we use $U_t - V^\pi(s_t; \theta_c)$ as an estimator for the advantage function $A(s, a) = Q^\pi(s, a) - V^\pi(s; \theta_c)$. As a result, the advantage function is given by

$$\begin{aligned} A(s_t, a_t) &= U_t - V^\pi(s_t; \theta_c) \\ &= \sum_{i=0}^{\tau-1} \gamma_i r(s_{t+i}, a_{t+i}) + \gamma_\tau V^\pi(s_{t+\tau}; \theta_c) - V^\pi(s_t; \theta_c). \end{aligned} \quad (29)$$

In the A3C framework, two loss functions are associated with the two deep neural network outputs of the actor network and the critic network. According to the advantage function (29), the actor loss function [31] under a given policy π is defined as

$$f_\pi(\theta_a) = \log \pi(a_t | s_t; \theta_a) (U_t - V^\pi(s_t; \theta_c)) + \vartheta G(\pi(s_t; \theta_a)), \quad (30)$$

where ϑ is a hyperparameter that controls the strength of the entropy regularization term, such as the exploration and exploitation management during the training process, and $G(\pi(s_t; \theta_a))$ is the entropy which is employed to favor exploration in training. From (30), the accumulated gradient of the actor loss function $f_\pi(\theta_a)$ is expressed as

$$d\theta_a = d\theta_a + \nabla_{\theta'_a} \log \pi(a_t | s_t; \theta'_a) (U_t - V^\pi(s_t; \theta_c)) + \vartheta \nabla_{\theta'_a} G(\pi(s_t; \theta'_a)), \quad (31)$$

where θ'_a is the thread-specific actor network parameters.

In addition, the critic loss function of the estimated value function is defined as

$$f(\theta_c) = (U_t - V^\pi(s_t; \theta_c))^2, \quad (32)$$

and the accumulated gradient of the critic loss function $f(\theta_c)$ in the critic network is calculated by

$$d\theta_c = d\theta_c + \frac{\partial (U_t - V^\pi(s_t; \theta_c))^2}{\partial \theta'_c}, \quad (33)$$

where θ'_c is the thread-specific critic network parameters.

After updating the accumulated gradients shown in (31) and (33), we adopt the standard non-centered RMSProp algorithm [32] to perform training for the loss function minimization in our presented A3C framework. The estimated gradient with the RMSProp algorithm of the actor or critic network is expressed as

$$g = \alpha g + (1 - \alpha)(\Delta\theta)^2, \quad (34)$$

where α denotes the momentum, and $\Delta\theta$ is the accumulated gradient ($d\theta_a$ or $d\theta_c$) of the actor loss function or the critic loss function. Note that the estimated gradient g can be either shared or separated across agent threads, but the shared mode tends to be more robust [31], [32]. The estimated gradient g is used to update the parameters of both the actor and critic networks as

$$\theta \leftarrow \theta - \beta \frac{\Delta\theta}{\sqrt{g + \varepsilon}}, \quad (35)$$

where β is the learning rate, and ε is a small positive step.

C. Training and Execution of A3C-AFL

Like most of machine learning algorithms, there are two stages in the proposed A3C-AFL algorithm, i.e., the training procedure and the execution procedure. Both the training and execution datasets are generated from their interaction of a federated learning environment conducted by the multi-UAV-enabled wireless network.

Algorithm 1 A3C-based Device Selection, UAVs Placement, and Resource Management

- 1: **Initialization:** Initialize the global parameters θ_a and θ_c of the actor and critic networks in the global network;
 Initialize the thread-specific parameters θ'_a and θ'_c in the local networks;
 Initialize the global shared counter $T = 0$ and thread counter $t = 1$ with the maximum counters T_{\max}^{A3C} and t_{\max}^{A3C} , respectively;
 - 2: Set $\alpha, \beta, \gamma, \varepsilon, T_{\max}^{\text{A3C}}$, and t_{\max}^{A3C} , respectively;
 - 3: **while** $T < T_{\max}^{\text{A3C}}$ **do**
 - 4: **for** each learning agent **do**
 - 5: Reset two accumulated gradients: $d\theta_a \leftarrow 0$ and $d\theta_c \leftarrow 0$;
 - 6: Synchronize thread-specific parameters $\theta'_a = \theta_a$ and $\theta'_c = \theta_c$;
 - 7: Set $t = t_0$ and observe a network state s_t ;
 - 8: **for** $t \leq t_{\max}^{\text{A3C}}$ **do**
 - 9: Select an action a_t based on the policy $\pi(a_t|s_t; \theta'_a)$;
 - 10: Receive an immediate reward r_t and observe a new reward s_{t+1} ;
 - 11: $t = t + 1$;
 - 12: **end for**
 - 13: Update the received return by

$$R_t = \begin{cases} 0, & \text{if } s_t \text{ is a terminal state,} \\ V^\pi(s_t; \theta_c), & \text{if } s_t \text{ is a non-terminal state.} \end{cases}$$
 - 14: **for** $i = t - 1$ to t_0 **do**
 - 15: $R = r_i + \gamma R_t$;
 - 16: Update the actor accumulative gradient $d\theta_a$ by using (31);
 - 17: Update the critic accumulative gradient $d\theta_c$ by using (33);
 - 18: Perform an asynchronous update of global parameters θ_a and θ_c based on (35), respectively;
 - 19: $T = T + 1$;
 - 20: **end for**
 - 21: **end while**
-

1. *The training procedure of A3C-AFL performs in an asynchronous way:*

- **The A3C Procedure:** The A3C algorithm is adopted for device selection, UAVs placement, and resource management in UAV-enabled networks, which is presented in **Algorithm 1**. The detailed processes of **Algorithm 1** are shown as follows. 1) Before training the A3C model, we load the real-world UAV-enabled network dataset and mobile devices' information, which generate a simulated environment for the federated learning scenario. 2) At the t -th global counter, the global A3C network parameters θ_a and θ_c as well as thread-specific parameters θ'_a and θ'_c are initialized. 3) Each UAV server acts as a learning agent to observe a network state s_t by interacting with the environment. 4) Each learning agent selects an action a_t (i.e.,

Algorithm 2 Asynchronous Federated Learning (AFL) Algorithm

1: **Input:** The maximum number of communication rounds T^{AFL} , client devices set \mathcal{K} , number of local iteration E^{AFL} per communication round, and learning rate η ;

Server process: // running at each UAV server

2: **Input:** Execute joint device selection, UAVs placement, and resource management by running **Algorithm 1**.

3: Initializes global model parameters $\mathbf{w}_n(0)$ at each UAV server $n \in \mathcal{N}$;

4: **for** each global round $t = 0, 1, 2, \dots, T^{\text{AFL}}$ **do**

5: **for** each UAV server $n = 0, 1, 2, \dots, N$ **do** in parallel

Device process: // running at each selected device

6: **for** each selected device $k \in \mathcal{K}_n$ in parallel **do**

7: Initialize $\mathbf{w}_k(t) = \mathbf{w}_n(t)$;

8: **for** $j = 0, 1, 2, \dots, E^{\text{AFL}}$ **do**

9: Sample $i \in \mathcal{D}_k$ uniformly at random and update the local parameters $\mathbf{w}_k(t)$ as follows

$$\mathbf{w}_k(t) = \mathbf{w}_n(t-1) - \eta \nabla F_k(\mathbf{w}_n(t-1));$$

10: **end for**

11: UAV server n collects the parameters $\{\mathbf{w}_k(t)\}_{k=1}^{K_n}$ from selected devices, and updates the global parameters

$$\mathbf{w}_n(t+1) = \sum_{k \in \mathcal{K}_n} |\mathcal{D}_k| \mathbf{w}_k(t) / |\mathcal{D}_n| ;$$

12: **end for**

13: **end for**

14: **Output:** Finalized global FL model parameters \mathbf{w}_n of each UAV server $n \in \mathcal{N}$.

device selection, UAVs placement, subchannel allocation, and power allocation) according to the policy probability distribution $\pi(a_t|s_t; \boldsymbol{\theta}'_a)$ in the actor network, and receives an immediate reward r_t as well as a new state s_{t+1} after executing the action a_t . 5) The state value function $V^\pi(s_t; \boldsymbol{\theta}'_c)$ and the estimation of advantage function $A(s_t, a_t)$ are updated in the critic network, and the probability distribution $\pi(a_t|s_t; \boldsymbol{\theta}'_a)$ is updated in actor network. 6) At each thread counter i , the accumulative gradients of the thread parameters $\boldsymbol{\theta}'_a$ and $\boldsymbol{\theta}'_c$ are updated according to (31) and (33), respectively. 7) The global network collects the parameters $d\boldsymbol{\theta}_a$ and $d\boldsymbol{\theta}_c$, then perform asynchronous update of the global parameters $\boldsymbol{\theta}_a$ and $\boldsymbol{\theta}_c$ by (35), before broadcasting them to each thread separately. 8) The A3C algorithm repeats the above training steps until the number of iterations gets the maximum global shared counter T_{\max}^{A3C} . Finally, the trained A3C model can be loaded to perform device selection, UAVs placement, and resource management for federated learning model updating.

- **The AFL Procedure:** This procedure consists of two phases, i.e., local training and global aggregation, which is provided in **Algorithm 2**. After performing **Algorithm 1**, the fol-

lowing procedure is implemented at each global communication round t for a federated learning system. 1) Each UAV sever n broadcasts its global model parameters $\mathbf{w}_n(t-1)$ to its associated devices, where the local model parameters at each participated device k is set as $\mathbf{w}_k(t) = \mathbf{w}_n(t-1)$, $k \in \mathcal{K}_n$. 2) In the n -th UAV-enabled cell, each selected device $k \in \mathcal{K}_n$ updates its local model parameters in an iterative manner according to the gradient of its loss function $F_k(\mathbf{w}_n(t-1))$. At each local iteration j , the local parameters $\mathbf{w}_k(t)$ are calculated by (20). 3) The K_n selected devices upload their updated local model-parameters $\{\mathbf{w}_k(t)\}_{k=1}^{K_n}$ to its associated UAV server n . 4) Each UAV server n aggregates the uploaded local model parameters from the K_n selected devices, and updates the global model parameters $\mathbf{w}_n(t)$ by (21) before broadcasting them to the associated devices.

2. Asynchronous Implementation of A3C-AFL:

We load the trained A3C model (i.e., **Algorithm 1**) to perform device selection, UAVs placement, and resource management in multi-UAV-enabled wireless networks. Then, the selected devices perform local training, and upload their local model-parameters to its associated UAV server over the allocated uplink subchannels. Each UAV server aggregates the collected local model parameters, and broadcasts the updated global model parameters to each associated device in the downlink. It is worth noting that the multiple agents (i.e., UAV servers) load their trained models (i.e., **Algorithm 1**) to asynchronously search for different exploration policies by interacting with their environment. In addition, the local model training is asynchronously executed among a range of participated devices, in order to enhance the efficiency of trained local models. Thus, to improve the federated aggregation efficiency, some model parameters update process of the associated devices may not be used for the global aggregation sometimes (i.e., **Algorithm 2**).

D. Complexity and Convergence Analysis

This subsection provides the computational complexity and convergence analysis of the proposed A3C algorithm for federated learning systems.

Let us define J and V as the number of DNN layers of the actor network and the critic network, respectively. Both the actor network and the critic network are also two fully connected networks. Define J_j as the number of neurons of the j -th layer in the actor network, and define V_i as the number of neurons of the i -th layer in the critic network. In the actor network, the computational complexity of the j -th layer is $O(J_{j-1}J_j + J_jJ_{j+1})$, and the total computational complexity with J layers is $O\left(\sum_{j=2}^{J-1}(J_{j-1}J_j + J_jJ_{j+1})\right)$. Similarly, in the critic network, the total computational complexity with V layers is $O\left(\sum_{i=2}^{V-1}(V_{i-1}V_i + V_iV_{i+1})\right)$. As the proposed

A3C algorithm is comprised of both the actor network and the critic network, the computational complexity of each training iteration is $O\left(\sum_{j=2}^{J-1}(J_{j-1}J_j + J_jJ_{j+1}) + \sum_{i=2}^{V-1}(V_{i-1}V_i + V_iV_{i+1})\right)$. We set that there have E episodes in the training phase, and each episode has T time steps. Thus, the overall computational complexity of the proposed A3C algorithm in the training process is $O\left(ET(\sum_{j=2}^{J-1}(J_{j-1}J_j + J_jJ_{j+1}) + \sum_{i=2}^{V-1}(V_{i-1}V_i + V_iV_{i+1}))\right)$.

Theorem 1: The A3C algorithm can reach convergence by using policy evaluation in the critic network and policy enhancement (the actor network) alternatively, i.e., $\pi(a_t|s_t; \theta_a) \in \Pi$ will converge to a policy $\pi^*(a_t|s_t; \theta_a)$ which guarantees $Q^{\pi^*}(s_t, a_t) > Q^\pi(s_t, a_t)$ for $\pi(a_t|s_t; \theta_a) \in \Pi$ and $(a_t, s_t) \in \mathcal{S} \times \mathcal{A}$, assuming $|\mathcal{A}| < \infty$. At the same time, it also requires to satisfy the following conditions [33], [34]: 1) the learning rates $\beta_a(t)$ and $\beta_c(t)$ of the actor network and critic network admit: $\sum_{t=0}^{\infty} \beta_a(t) = \infty$, $\sum_{t=0}^{\infty} \beta_a^2(t) < \infty$, $\sum_{t=0}^{\infty} \beta_c(t) = \infty$, $\sum_{t=0}^{\infty} \beta_c^2(t) < \infty$, and $\lim_{t \rightarrow \infty} \beta_a(t)/\beta_c(t) = 0$; 2) The instantaneous reward $\text{Var}\{r_t\}$ is bounded; 3) The policy function $\pi(a|s; \theta_a)$ is continuously differentiable in θ_a ; 4) The sequence (a_t, s_t, r_t) is Independent and identically distributed (i.i.d.), and has uniformly bounded second moments [33], [34].

Proof: See Appendix A.

In the following, we discuss the convergence property of the FL algorithm. Let us define the upper bound of the divergence between the federated loss function $F(\mathbf{w})$ and the global optimal loss function $F(\mathbf{w}^*)$ as $|F(\mathbf{w}) - F(\mathbf{w}^*)|$, where \mathbf{w}^* is the global optimal parameters.

Definition 1: The FL algorithm can achieve the global optimal convergence if it satisfies [10], [11]

$$|F(\mathbf{w}) - F(\mathbf{w}^*)| \leq \varepsilon, \quad (36)$$

where ε is a small positive constant $\varepsilon > 0$.

Theorem 2: When $F(\mathbf{w})$ is a η -convex and σ -smooth function, the upper bound of $[F(\mathbf{w}) - F(\mathbf{w}^*)]$ can be expressed

$$F(\mathbf{w}) - F(\mathbf{w}^*) \leq \varepsilon (F(\mathbf{w}(0)) - F(\mathbf{w}^*)). \quad (37)$$

Proof: The details of the proof can be seen in [10], [11].

For appropriate selections of the iteration numbers, i.e., the global iterations T^{AFL} and the local iterations E^{AFL} , the FL algorithm will finally coverage to the global optimality (36), the more proof analysis can be found in [10], [11].

IV. SIMULATION RESULTS AND ANALYSIS

In this section, we evaluate the performance of our proposed A3C-AFL algorithm under different parameter settings. In our simulations, the performance is evaluated in the Python 3

environment on a PC with Intel (R) Core(TM) i7-6700 CPU @ 3.40 GHz, 16 RAM, and the operating system is Windows 10 Ultimate 64 bits. We also compare the performance of the following different algorithms/approaches:

1) *AFL with device selection*: Proposed asynchronous federated learning framework with adopting device selection strategy (i.e., high communication and computation capabilities) to perform model aggregation.

2) *AFL without device selection*: Proposed asynchronous federated learning framework with adopting random device selection strategy to perform model aggregation [17].

3) *SFL with device selection*: Synchronous federated learning framework with adopting device selection strategy to perform model aggregation [20].

4) *A3C-AFL*: Adopting proposed A3C to perform device selection, UAVs placement, and resource management in the asynchronous federated learning framework.

5) *A3C-SFL*: Adopting proposed A3C to perform device selection, UAVs placement, and resource management in the synchronous federated learning framework.

6) *Gradient-AFL*: Adopting gradient-based benchmark to perform device selection, UAVs placement, and resource management in the asynchronous federated learning framework.

For our simulations, we consider a multi-UAV-enabled network where four UAVs are deployed in the sky to support the coverage of a square area of $400 \text{ m} \times 400 \text{ m}$. At the beginning, four UAVs are uniformly located in the sky at the height of 150 m. The device training data of each device k follows uniform distribution [5,10] Mbits, and the CPU computation capacity of the devices range from 1.0 GHz to 2.0 GHz. The transmit power of each device is set to be equal to 50 mW, and the maximum transmit power of each UAV is 150 mW. The transmit data size of model parameters is 200 kbits, and the weight parameter is $\lambda = 0.4$ in (19). Both the actor network and the critic network are conducted with deep neural networks (DNNs), and they have three hidden fully-connected layers. Each of the layers in the actor network or the critic network contains 256 neurons, 256 neurons, and 128 neurons, respectively. The actor network is trained with the earning rate 0.0001, and the critic network is trained with the learning rate 0.001 [33], [34]. The discount factor is $\gamma = 0.98$. We evaluate the proposed AFL on the MNIST dataset [15], [16], and the Convolutional Neural Network (CNN) tool is used to train the local model. In each global communication round, FL has one global aggregation and 10 iterations for local training. The relevant simulation parameters are provided in Table I.

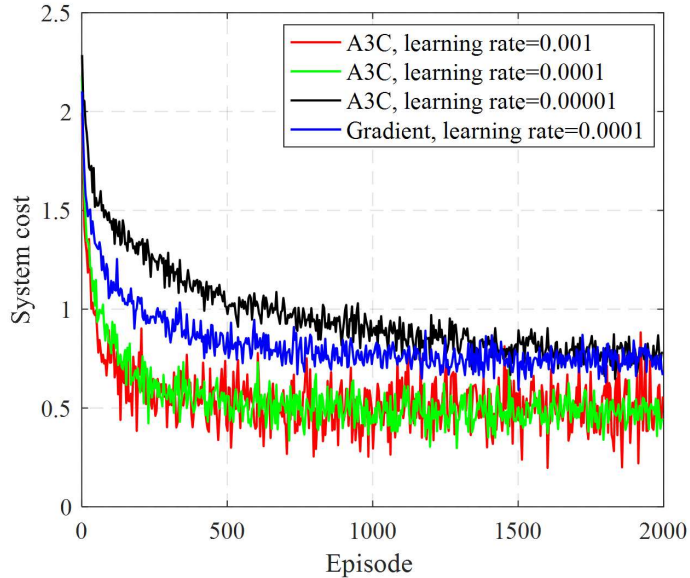


Fig. 3. Training convergence of A3C-based learning algorithm in terms of the system cost.

A. Convergence Comparison of Algorithms

We first evaluate the convergence of the proposed A3C-based learning algorithm with the different learning rates of the actor network, i.e., $\beta_a = \{0.001, 0.0001, 0.00001\}$, and also compare it with the gradient-based benchmark algorithm. Note that the system cost is the objective function in (19), which includes the model aggregation time and the learning accuracy loss. The learning rate of DNN plays a key role on the convergence speed and system cost. From Fig. 3, we can observe that a large value of learning rate (i.e., $\beta_a = 0.001$) may cause oscillations while a small value of the learning rate (i.e., $\beta_a = 0.00001$) produces slow convergence. Hence, we select a suitable learning rate, neither too large nor too small, and the value can be set around 0.0001 in the training model, which can guarantee the fast convergence speed and the low system cost. In addition, it is interesting to note that both the proposed A3C-based learning algorithm and the gradient-based benchmark algorithm have the comparable convergence speed, and when the training episode approximately reaches 500, the system cost gradually converges despite some fluctuations due to dynamic environment characteristic and policy exploration. However, our proposed algorithm achieves the lower system cost than that of the gradient-based benchmark algorithm. In addition, we also carry out a test and trials for the critic's learning rate selection, where the learning rate of the critic network is selected at 0.001 which has high convergence speed and low system cost [33], [34].

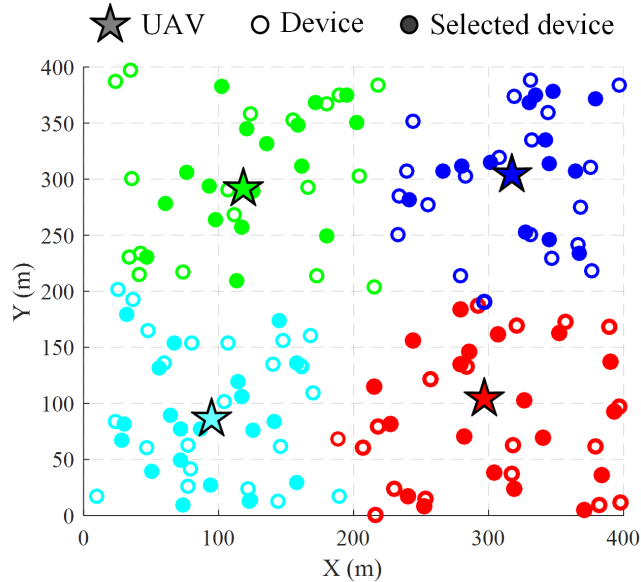


Fig. 4. Two dimensional distribution of UAVs, ground devices and participated devices.

B. UAVs Placement and Device Selection Evaluation

Figure 4 captures the 2D deployment of the UAVs (in a horizontal plane) and selected devices distribution in one time slot, where a number of $K=150$ devices are randomly located over the coverage areas of their associated UAVs. UAVs adaptively update their locations according to the number of associated devices and devices' distributions, in order to provide the best channel gain and minimize the communication delay between UAVs and the devices. It is worth noting that a part of devices with high communication and computation capabilities (solid dots) are selected to participate the FL model aggregation, to minimize the aggregation time and learning accuracy loss, while the remaining low-quality devices (hollow dots) don't participate in the FL model aggregation in this time slot.

C. Accuracy Comparison with Different Global Rounds and Implementation Time

In Fig. 5, we compare the accuracy performance versus the number of global rounds and wall-clock time for different FL approaches, where several devices are set as low-quality participants. The low-quality participants are with low communication and computation capabilities, and even have low-quality training parameters [14]. From Fig. 5(a), we can observe that both the AFL and SFL approaches with device selection requires about 25 global rounds to achieve an accuracy of 90.0%, and both of them have similar convergence speed and accuracy performance. However, at each global round, SFL has to wait until all the selected devices response, while AFL only

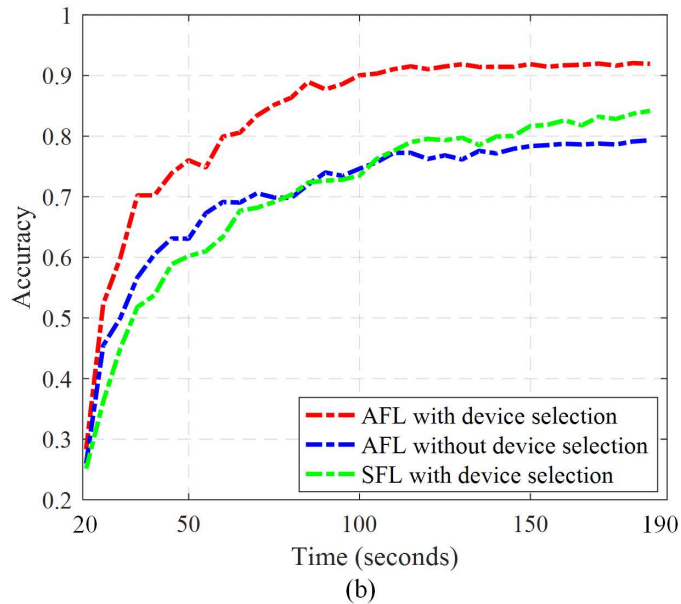
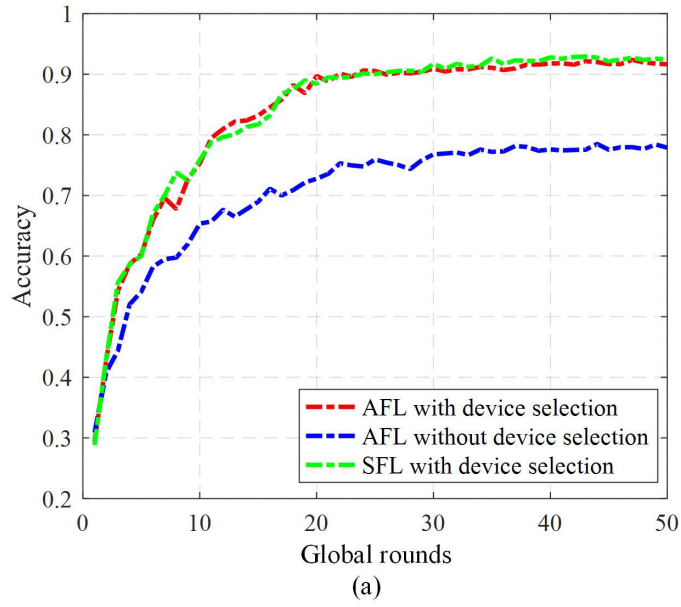


Fig. 5. Accuracy comparison versus (a) number of global communication rounds and (b) wall-clock time.

needs a number of selected devices' response to move on to the next round which decreases the aggregation completion time during the learning process as shown in Fig. 5(b). In addition, both the AFL and SFL approaches with device selection achieve higher accuracy and convergence speed than those of the AFL approach without device selection. The results illustrate that the proposed device selection scheme can prevent low-quality devices from affecting the learning accuracy, and enhances the system performance significantly.

From Fig. 5(b), we can see that the accuracy of all approaches improves with the increase of the wall-clock time. However, by comparing different approaches, the proposed AFL approach with device selection outperforms the other two approaches in terms of both the convergence speed and accuracy. The reason lies on the fact that the AFL approach without device selection may enable the low-quality devices to participate in the FL model aggregation, where the low-quality model parameters decrease the overall accuracy, as well as devices with low communication and computation capacities need more time to complete the model aggregation. In addition, the SFL approach with device selection has to wait for all selected devices to complete their local model parameters update, among which there may require long computation time due to low computation capability. Consequently, each global communication round of the SFL approach with device selection requires more time to finish model aggregation, and hence its accuracy performance slowly improves with the increase of wall-clock time. The results from Fig. 5 demonstrate that the proposed AFL approach with device selection is capable of improving both the convergence speed and aggregation accuracy performance.

D. Performance Comparison Versus Number of Devices

Figure 6 presents the aggregation accuracy and completion time achieved by different algorithms with various numbers of devices. As we can see from Fig. 6(a), the proposed A3C-AFL and A3C-SFL algorithms achieve the superior accuracy compared to the AFL without device selection algorithm under different numbers of devices, and the advantage gap becomes large with the increase of the devices. The reason is that the devices with low-quality model parameters in the AFL without device algorithm compromise the accuracy after model aggregation, while the proposed A3C algorithm selects the devices with high-quality model parameters for model aggregation which can significantly improve the overall accuracy. Furthermore, the accuracy of the A3C algorithm increases with the increase of devices, because the network has the more probability of searching participated devices having high-quality model parameters to enhance the aggregation accuracy. However, the accuracy of the AFL without device selection algorithm maintains at a horizontal level (i.e., about 78.0%) with some fluctuation during this process, since it doesn't keep the low-quality devices from decreasing the aggregation accuracy. In addition, the accuracy performance of the gradient-AFL algorithm increases with K , but it has a lower accuracy than that of the proposed A3C-AFL algorithm.

Fig. 6(b) illustrates that the aggregation completion time of the A3C-SFL and AFL without device selection algorithms increases with the increase of devices, while the A3C-AFL and gradient-AFL algorithms decrease slightly during this process. Generally, the more devices

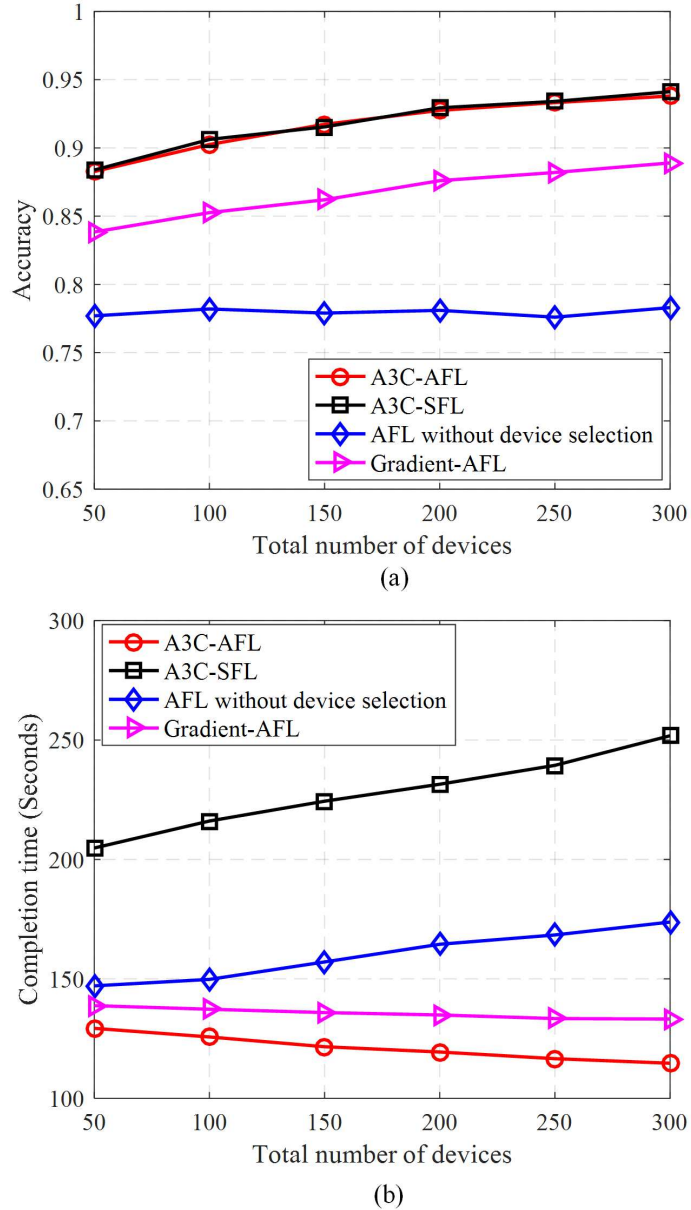


Fig. 6. (a) Accuracy and (b) aggregation completion time comparisons versus total number of devices K .

there are, the more completion time is required to learn the optimal solution for the A3C-SFL algorithm. The reason is that SFL needs to wait for all selected devices to complete their local parameters update before aggregating the local models at each communication round. In addition, for the AFL without device selection algorithm, as more devices participate in the model aggregation, the participated devices with low-quality computation and communication capabilities consume longer time for global model aggregation. Even though the gradient-AFL algorithm prevents low-quality devices from increasing the completion time, it needs more time

to complete the decision making compared to the A3C-AFL algorithm. The results show that the proposed A3C algorithm can carry out the better decision making for the device selection, UAVs placement, and resource management than that of the gradient-based benchmark.

V. CONCLUSIONS

This paper has investigated how to minimize the execution time and learning accuracy loss of privacy-preserving federated learning in multi-UAV-enabled wireless networks. Specifically, an AFL framework was proposed to provide asynchronous distributed computing by enabling model training locally without transmitting raw sensitive data to UAV servers. The device selection strategy was also introduced into the AFL framework to select the mobile devices with high communication and computation capabilities to improve the learning efficiency and accuracy. Moreover, we also proposed an A3C-based joint device selection, UAVs placement, and resource management algorithm to enhance the learning convergence speed and accuracy. Simulation results have demonstrated that the proposed AFL framework with A3C-based algorithm outperform the existing solutions in terms of learning accuracy and execution time under different settings.

APPENDIX A PROOF OF THEOREM 1

For all agents (i.e., UAV servers) in the environment, the network aims to search a joint policy in the coordinated multi-agent RL scenario, where the joint policy can be expressed as

$$\pi(s|a) = \begin{bmatrix} \pi^1(s^1|a^1) \\ \vdots \\ \pi^N(s^N|a^N) \end{bmatrix} = \begin{bmatrix} \arg \max_{a^1 \in \mathcal{A}_1} Q^1(s^1|a^1) \\ \vdots \\ \arg \max_{a^N \in \mathcal{A}_N} Q^N(s^N|a^N) \end{bmatrix}, \quad (38)$$

where s^n , a^n , and \mathcal{A}_n denote the individual state, action and action space of the n -th agent.

As A3C uses the policy evaluation in the critic network and policy enhancement in the actor network alternatively, we adopt the two-time-scale stochastic approximation [33], [34] to provide the convergence proof analysis of A3C. In detail, the convergence of the critic network is first analyzed with the joint policy $\pi(s|a)$ being fixed. Then, we provide the convergence analysis of the policy parameter θ_a upon the convergence of the actor network.

Here, let us define the transition probability of state-action pair as $\mathcal{T}(s', a'|s, a) = \mathcal{T}(s'|s, a)\pi(s'|a')$ and the stationary distribution of MDP as $D(s, a) = \text{diag}[d(s) \cdot \pi(s|a)]$, $s \in \mathcal{S}, a \in \mathcal{A}$, where $d(s)$ denotes the stationary distribution of the Markov chain induced by policy $\pi(s|a)$. The sum

cumulative reward of all agents is expressed as $\bar{U}(s, a) = \sum_{n \in \mathcal{N}} U_n(s, a)$, and the overall available cumulative reward set in learning process is defined as $\hat{U}(s, a) \equiv [\bar{U}(s, a), s \in \mathcal{S}, a \in \mathcal{A}]$. The joint long-term return under the joint policy $\pi(s|a)$ is expressed as

$$J(\boldsymbol{\theta}) = \sum_{s \in \mathcal{S}} d(s) \sum_{a \in \mathcal{A}} \pi(s|a) \hat{U}(s, a). \quad (39)$$

In addition, the operator W^Q for any action-value function $Q(s, a; \boldsymbol{\theta}_c)$ is defined as [33], [34]

In A3C, the action-value function can be expressed by using the linear functions [33], [34], i.e., $Q(s, a; \boldsymbol{\theta}_c) = \boldsymbol{\theta}_c^T \cdot \boldsymbol{\Psi}(s, a)$, where $\boldsymbol{\Psi}(s, a) = (\psi_1(s, a), \psi_2(s, a), \dots, \psi_{|\mathcal{S}|}(s, a))^T$ is the feature vector (basis function vector) at the state s . The critic network aims to find a unique solution $\boldsymbol{\theta}_c$ by satisfying

$$\boldsymbol{\Psi}(s, a) \cdot D(s, a) [W^Q(\boldsymbol{\theta}_c^T \cdot \boldsymbol{\Psi}(s, a)) - \boldsymbol{\theta}_c^T \cdot \boldsymbol{\Psi}(s, a)] = 0. \quad (40)$$

As the solution to (41) is a limiting point of the $TD(0)$ method, and thus we approximate the action-value function $Q(s, a; \boldsymbol{\theta}_c)$ instead of the state-value function $V(s, a; \boldsymbol{\theta}_c)$. This solution can be achieved by minimizing the Mean Square Projected Bellman Error, i.e.,

$$\min_{\boldsymbol{\theta}_c} \left\| \boldsymbol{\theta}_c^T \cdot \boldsymbol{\Psi}(s, a) - \Pi(W^Q(\boldsymbol{\theta}_c^T \cdot \boldsymbol{\Psi}(s, a))) \right\|_{D(s, a)}^2, \quad (41)$$

where $\Pi(\cdot)$ denotes the operator that projects a vector to the space, and $\|\cdot\|_{D(s, a)}$ is the Euclidean norm. In the coordinated scenario, each agent exchanges its decisions with each other, and all of them will achieve a copy of the estimation of the jointly averaged action-value function, i.e., $\boldsymbol{\theta}_c^n \rightarrow \boldsymbol{\theta}_c$ for all $n \in \mathcal{N}$. The joint action $a = \langle a_1, \dots, a_N \rangle$ of A3C in state s is in a global point that all agents coordinately achieve the sum highest return from the environment, i.e., $a = \arg \max_{a \in \mathcal{A}} Q(s, a; \boldsymbol{\theta}_c)$. In other words, the final critic parameter $\boldsymbol{\theta}_c$ is achieved by iteratively minimizing (42), and the Q value will converge to the final point Q^* with probability 1 [33], [34].

To analyze the convergence of the actor network, the advantage function of the n -th agent in (29) is rewritten as

$$A_t^n(s, a) = \boldsymbol{\theta}_c^T \cdot \boldsymbol{\Psi}(s, a) - \sum_{a^n \in \mathcal{A}^n} \pi^n(s_t, a^n) \cdot \boldsymbol{\theta}_c^T \cdot \boldsymbol{\Psi}(s, a). \quad (42)$$

Using Assumptions 2.2 and 4.1-4.5 [34], for the n -th agent, the policy parameter $\boldsymbol{\theta}_a^n$ of the actor network in (35) will converge to a point from the following set of asymptotically stable equilibria of

$$\boldsymbol{\theta}_a^n = \Gamma^n \left[\mathbb{E}_{s_t \sim d(s), a_t \sim \pi} \left(A_t^n(s, a) \cdot \nabla_{\boldsymbol{\theta}_a^n} \log \pi^n(s|a^n) \right) \right], \text{ for } n \in \mathcal{N}, \quad (43)$$

where $\Gamma[\cdot]$ denotes an operator that projects any vector onto the compact set. The estimation of the policy gradient $A_t^n(s, a) \cdot \nabla_{\theta_a^n} \log \pi^n(s|a^n)$ satisfies

$$\begin{aligned} & \mathbb{E}_{s_t \sim d(s), a_t \sim \pi} (A_t^n(s, a) \cdot \nabla_{\theta_a^n} \log \pi^n(s|a^n)) \\ &= \nabla_{\theta_c^n} J(\theta) + \mathbb{E}_{s_t \sim d(s), a_t \sim \pi} ((Q(s, a; \theta_c) - \theta_c^T \cdot \Psi(s, a)) \cdot \nabla_{\theta_a^n} \log \pi^n(s|a^n)). \end{aligned} \quad (44)$$

As the linear features here are not limited by the compatible features, we can get the convergence to the stationary point of $\mathbb{E}_{s_t \sim d(s), a_t \sim \pi} (A_t^n(s, a) \cdot \nabla_{\theta_a^n} \log \pi^n(s|a^n)) = 0$ in the set of the policy parameters. In this case, when the long-term averaged return $J(\theta)$ satisfies $\nabla_{\theta_c^n} J(\theta) = 0$, the error between the approximation function $\theta_c^T \cdot \Psi(s, a)$ and the action value function $Q(s, a; \theta_c)$ is small, i.e., $Q(s, a; \theta_c) - \theta_c^T \cdot \Psi(s, a) \approx 0$. Thus, we can achieve the best solution for A3C with general linear function approximation [33], [34]. Due to the update rule in (45) and the coordination nature of the coordinated multi-agent A3C, a joint policy π implied by multiple policies is updated by each agent, eventually converges to the final point. The more details of the proof can be seen in [33], [34].

REFERENCES

- [1] X. Lu, L. Xiao, C. Dai, and H. Dai, "UAV-aided cellular communications with deep reinforcement Learning Against Jamming," *IEEE Wireless Commun.*, vol. 27, no. 4, pp. 48-53, Aug. 2020.
- [2] F. Qi, X. Zhu, G. Mang, M. Kadoch, and W. Li, "UAV network and IoT in the sky for future smart cities," *IEEE Network*, vol. 33, no. 2, pp. 96-101, Mar. 2019.
- [3] Y. Zeng, Q. Wu, and R. Zhang, "Accessing from the sky: A tutorial on UAV communications for 5G and beyond," *Proc. of IEEE*, vol. 107, no. 12, pp. 2327-2375, Dec. 2019.
- [4] B. Brik, A. Ksentini, and M. Bouaziz, "Federated learning for UAV-enabled wireless networks: Use cases, challenges, and open problems," *IEEE Access*, pp.53841-53849, May 2020.
- [5] J. Konecny, H. B. McMahan, F. X. Yu, P. Richtrik, A. T. Suresh, and D. Bacon, "Federated learning: Strategies for improving communication efficiency, 2016. [Online]. Available: <https://arxiv.org/abs/1610.05492>.
- [6] H. B. McMahan *et al.*, "Communication-efficient learning of deep networks from decentralized data," in *Proc. 20th Int. Conf. Artif. Intell. Stat.*, Fort Lauderdale, FL, USA, Apr. 2017, vol. 54, pp. 1273–1282.
- [7] S. Ruder, "An overview of gradient descent optimization algorithms," 2016. [Online]. Available: <https://arxiv.org/abs/1609.04747>.
- [8] T. Zeng, O. Semiari, M. Mozaffari, M. Chen, W. Saad, and M. Bennis, "Federated learning in the sky: Joint power allocation and scheduling with UAV swarms," CoRR abs/2002.08196, 2020.
- [9] H. Shiri, J. Park, and M. Bennis, "Communication-efficient massive UAV online path control: Federated learning meets mean-field game theory, CoRR abs/2003.04451, 2020.
- [10] N. H. Tran, W. Bao, A. Zomaya, and C. S. Hong, "Federated learning over wireless networks: Optimization model design and analysis," in *Proc. IEEE INFOCOM*, Paris, France, 2019, pp. 1387–1395.
- [11] S. Wang, T. Tuor, T. Salonidis, K. K. Leung, C. Makaya, T. He, and K. Chan, "Adaptive federated learning in resource constrained edge computing systems," *IEEE J. Sel. Areas Commun.*, vol. 37, no. 6, pp. 1205–1221, 2019.
- [12] S. Wang *et al.*, "When edge meets learning: Adaptive control for resource-constrained distributed machine learning," in *Proc. Int. Conf. Comput. Commun. (INFOCOM)*, Honolulu, HI, 2018, pp. 63-71.

- [13] H. H. Yang, Z. Liu, T. Q. S. Quek, and H. V. Poor, "Scheduling policies for federated learning in wireless networks," *IEEE Trans. Commun.*, vol. 68, no. 1, pp. 317-333, Jan. 2020.
- [14] Y. Lu, X. Huang, K. Zhang, S. Maharjan, and Y. Zhang, "Blockchain empowered asynchronous federated learning for secure data sharing in internet of vehicles," *IEEE Trans. Veh. Technol.*, vol. 69, no. 4, pp. 4298-4311, Apr. 2020.
- [15] S. Luo, X. Chen, Q. Wu, Z. Zhou, and S. Yu, "HFEL: Joint edge association and resource allocation for cost-efficient hierarchical federated edge learning," to appear in *IEEE Trans. Wireless Commun.*, doi: 10.1109/TWC.2020.3003744.
- [16] T. Nishio and R. Yonetani, "Client selection for federated learning with heterogeneous resources in mobile edge," in *Proc. IEEE Int. Conf. Commun. (ICC)*, Shanghai, China, 2019, pp. 1-7.
- [17] Y. Chen, X. Sun, and Y. Jin, "Communication-efficient federated deep learning With layerwise asynchronous model update and temporally weighted aggregation," to appear in *IEEE Trans. Neural Netw. Learn. Syst.*, doi: 10.1109/TNNLS.2019.2953131.
- [18] Y. Liu, J. Nie, X. Li, S. H. Ahmed, W. Yang B. Lim, and C. Miao, "Federated learning in the sky: Aerial-ground air quality sensing framework with UAV swarms," 2020. [Online]. Available: <https://arxiv.org/abs/2007.12004>.
- [19] W. Y. B. Lim, J. Huang, Z. Xiong, J. Kang, D. Niyato, X.-S. Hua, C. Leung, and C. Miao, "Towards federated learning in UAV-enabled Internet of vehicles: A multi-dimensional contact-matching approach," CoRR abs/2004.03877, 2020.
- [20] J. S. Ng *et al.*, "Joint auction-coalition formation framework for communication-efficient federated learning in UAV-enabled Internet of Vehicles," 2020. [Online]. Available: <https://arxiv.org/abs/2007.06378>.
- [21] Z. M. Fadlullah and N. Kato, "HCP: Heterogeneous computing platform for federated learning based collaborative content caching towards 6G networks," to appear in *IEEE Trans. Emerging Topics in Comput.*, doi: 10.1109/TETC.2020.2986238.
- [22] Y. Wang, Z. Su, N. Zhang, and A. Benslimane, "Learning in the air: Secure federated Learning for UAV-assisted crowdsensing," to appear in *IEEE Trans. Netw. Sci. Eng.*, doi: 10.1109/TNSE.2020.3014385.
- [23] Q. Wu, Y. Zeng, and R. Zhang, "Joint trajectory and communication design for multi-UAV enabled wireless networks," *IEEE Trans. Wireless Commun.*, vol. 17, no. 3, pp. 2109-2121, Mar. 2018.
- [24] S. Yin, L. Li, and F. R. Yu, "Resource allocation and base station placement in downlink cellular networks assisted by multiple wireless powered UAVs," *IEEE Trans. Veh. Technol.*, vol. 69, no. 2, pp. 2171-2184, Feb. 2020
- [25] Y. Zhang, Z. Mou, F. Gao, J. Jiang, R. Ding, and Z. Han, "UAV-enabled secure communications by multi-agent deep reinforcement learning," to appear in *IEEE Trans. Veh. Technol.*, doi: 10.1109/TVT.2020.3014788.
- [26] N. Zhao, Z. Liu, and Y. Cheng, "Multi-agent deep reinforcement learning for trajectory design and power allocation in multi-UAV networks," *IEEE Access*, vol. 8, pp. 139670-139679, 2020.
- [27] M. Zhu, X. Liu, and X. Wang, "Deep reinforcement learning for unmanned aerial vehicle-assisted vehicular networks," 2019, [Online]. Available: <https://arxiv.org/abs/1906.05015>.
- [28] L. Wang, K. Wang, C. Pan, W. Xu, N. Aslam, and A. Nallanathan, "Deep reinforcement learning based dynamic trajectory control for UAV-assisted mobile edge computing," 2019, [Online]. Available: <https://arxiv.org/abs/1911.03887>.
- [29] A. Al-Hourani, S. Kandeepan, and S. Lardner, "Optimal LAP altitude for maximum coverage," *IEEE Wireless Commun. Lett.*, vol. 3, no. 6, pp. 569-572, Dec. 2014.
- [30] Richard S. Sutton, Andrew G. Barto. Introduction to reinforcement learning, 1st MIT Press Cambridge, MA, USA, 1998.
- [31] V. Mnih, A. P. Badia, M. Mirza, A. Graves, T. Lillicrap, T. Harley, D. Silver, and K. Kavukcuoglu, "Asynchronous methods for deep reinforcement learning," in *Proc. Int. Conf. Machine Learn.*, 2016, pp. 1928-1937.

- [32] T. Tijmen and H. Geoffrey. Lecture 6.5-rmsprop: Divide the gradient by a running average of its recent magnitude. COURSERA: *Neural Networks for Machine Learn.*, 4, 2012.
- [33] T. Haarnoja, A. Zhou, P. Abbeel, and S. Levine, “Soft actor-critic: Off policy maximum entropy deep reinforcement learning with a stochastic actor,” *CoRR*, vol. abs/1801.01290, pp. 1–15, 2018.
- [34] K. Q. Zhang, Z. R. Yang, H. Liu, T. Zhang, and T. Ba?ar, “Fully decentralized multi-agent reinforcement learning with networked agents,” 2018, [Online]. Available: <https://arxiv.org/abs/1802.08757>.